Supporting Information

Verheijen et al. 10.1073/pnas.0905633106

SI Text

Microdissection of Sciatic Nerve. Sciatic nerves from adult (P56 and P210) mice were placed in ice-cold PBS (pH 7.4). The perineurium and epineurium were gently dissected away from the endoneurium along the whole length of the nerve as described in ref. 1.

Quantitative PCR. Total RNA from rat primary Schwann cells was isolated by using TRIzol (Invitrogen), total RNA from complete sciatic nerve (P0, P4, and P8) or endoneurium (P56, and P210) was isolated by using the Qiagen RNeasy lipid tissue kit (Qiagen) following the manufacturer's instructions. cDNA synthesis and quantitative PCR reactions were done as described (2, 3). Results were normalized by using the reference genes cyclophilin or ubiquitin. All primer sequences are in Table S1.

Electron Microscopy and Morphometric Analysis. Sciatic nerves of pups (P0, P4, or P10) were isolated and immersion-fixed in 4% paraformaldehyde/PBS for 2 h. Adult mice (P56 and P210) were perfused with 4% paraformaldehyde/PBS for 20 min. Nerves were postfixed in 2.5% glutaraldehyde in 0.05 M sodium cacodylate buffer for 2 h, rinsed in 0.1 M sodium cacodylate, and osmicated for 1.5 h (in 1% OsO_4, 1.5% $K3Fe(CN)_6$, and 2% sucrose). Nerves were dehydrated in ethanol and embedded in Epon. Ultra-thin sections were subsequently cut, collected on formvar coated single slot grids, and stained with a 1% aqueous uranyl acetate solution for 20 min and subsequently for 1 min with lead citrate. Photographs were obtained by using a JEOL 1010 electron microscope. For each myelinated axon present, at P10 and P210, the g-ratio was calculated by dividing the axonal diameter (defined by the inner limit of the myelin sheath), by the total fiber diameter (defined by the outer limit of the myelin sheath). Each group consisted of at least three mice.

Cell Culture, Transfections, and Luciferase Assays. Isolation of primary rat Schwann cells, transfections of plasmids using Geneporter, and luciferase assays were done as described in ref. 12. Transfections of siRNAs (Dharmacon) were done for 6 h in antibiotic-free medium by using the cationic lipid DharmaFECT 3 (Dharmacon) following manufacturer instructions. SiRNAs against SCAP (ON-TARGET plus SMART pool of four siRNAs), nontargeting siRNA (ON-TARGET plus siCONTROL pool of 4 siRNAs), or nontargeting fluorescent and impaired ability for RISC interaction siRNA (siGLOW RISC-Free) were used. Twenty-four hours after transfection, mRNA-knockdown was determined by using PCR as described above.

Western Blot Analysis. Preparation of protein lysates of mouse sciatic endoneurium and immunoblotting was performed as described in ref. 10. Detection of SCAP was done by using goat anti-SCAP (1:100; Santa Cruz), and detection of SREBP1 was done by using 2A4 mouse anti-SREBP1 (1:200, Santa Cruz). Immunoblots were re-probed with mouse anti-β-actin antibodies to control for protein loading.

1. Verheijen MH, Chrast R, Burrola P, Lenke G (2003) Local regulation of fat metabolism in peripheral nerves. *Genes Dev* 1719:2450–2464.
2. de Preux AS, et al. (2007) SREBP-1c expression in Schwann cells is affected by diabetes and nutritional status. *Mol Cell Neurosci* 354:525–534.
3. Nadra K, et al. (2008) Phosphatidic acid mediates demyelination in Lpin1 mutant mice. *Genes Dev* 2212:1647–1661.

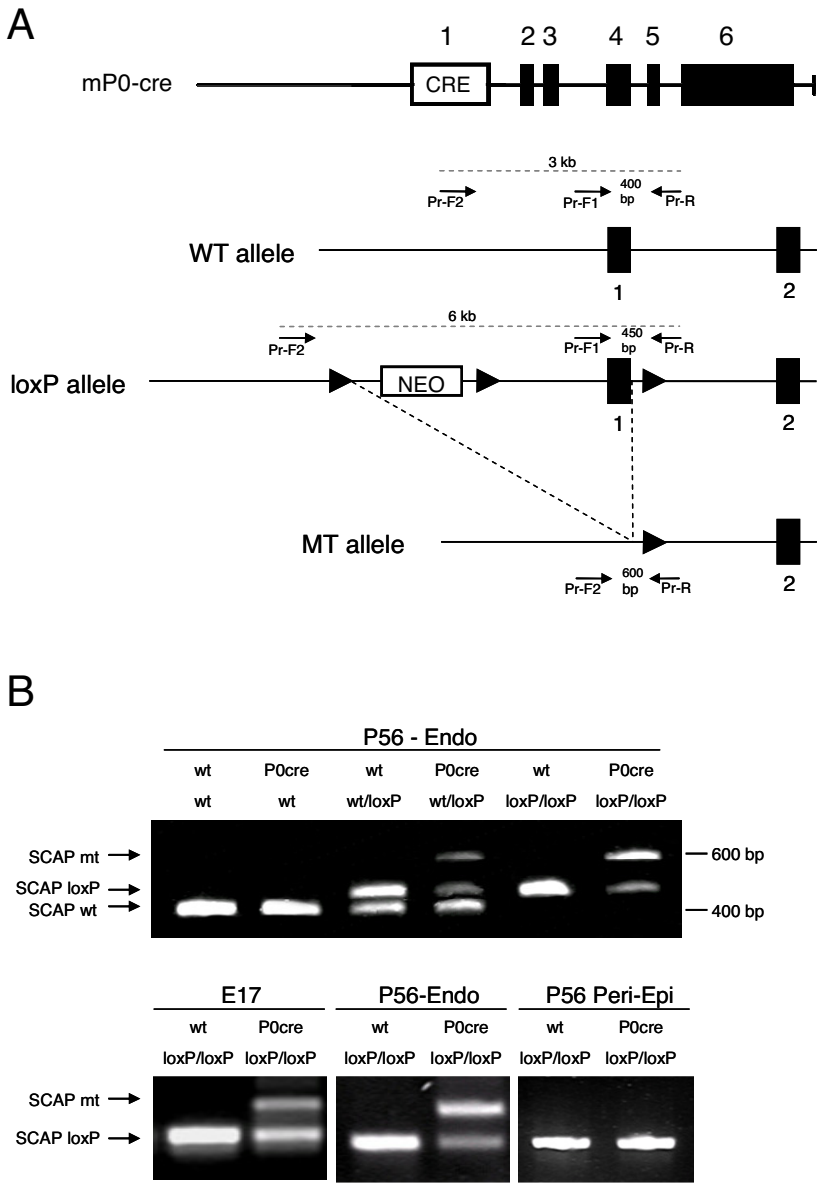

Fig. S1. Generation of Schwann cell specific SCAP mutant mice. (*A*) Schematic presentation of the mouse P0cre (mP0-cre) transgene containing the Cre gene inserted into exon 1 of the MPZ gene, and the SCAP wild-type (WT) allele, the SCAP loxP targeted allele, and the SCAP mutant (MT) allele in which exon 1 and the neo cassette are deleted after cre-mediated recombination. (*B*) PCR analysis of SCAP alleles on genomic DNA isolated from P56 sciatic nerve endoneurium (endo), E17 sciatic nerve, or P56 sciatic nerve perineurium/epineurium (peri/epi), from animals being P0cre transgene positive (P0cre) or negative (wt), and wild-type (wt) or either heterozygous (wt/loxP) or homozygous (loxP/loxP) for the SCAP loxP allele. A mixture of three primers was used. The F1/R primer pair gives a product of 400-bp for the SCAP wild-type allele and a 450-bp product for the SCAP loxP allele. Recombination-mediated deletion of the neo cassette and exon 1 allows the F2/R primer pair to amplify a product of 600-bp for the mutant allele.

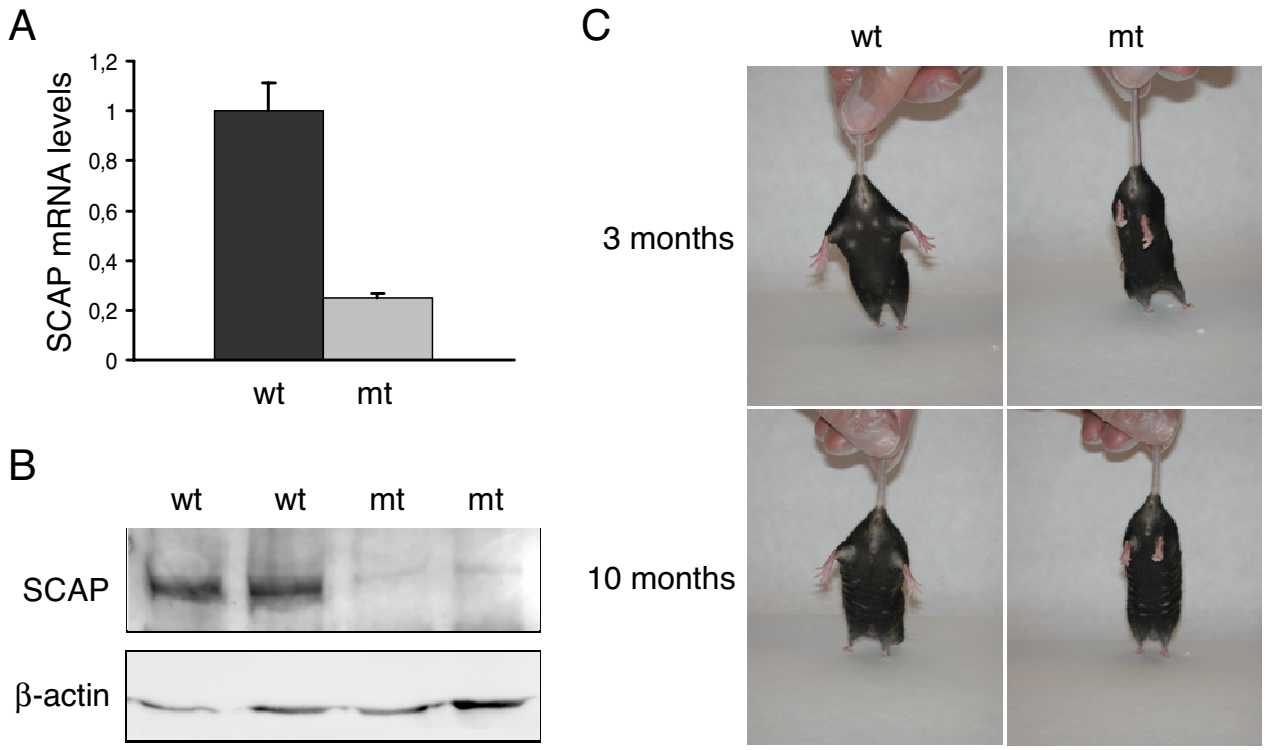

Fig. S2. Conditional inactivation of SCAP in Schwann cells leads to peripheral nerve impairment. (*A*) Quantitative PCR analysis of SCAP mRNA levels in sciatic nerve endoneurium of wild-type (wt) versus mutant (mt) adult (P56) mice. The data represent the mean ± standard deviation of triplicate measurements. (*B*) Immunoblot analysis of the SCAP protein in sciatic nerve endoneurium from two wild-type and two mutant (P56) mice. β-actin was used to control for equal protein loading. (*C*) When lifted by the tail, mutant mice show an abnormal reaction by clenching the toes of their rear feet and attempting to clasp their hind limbs together.

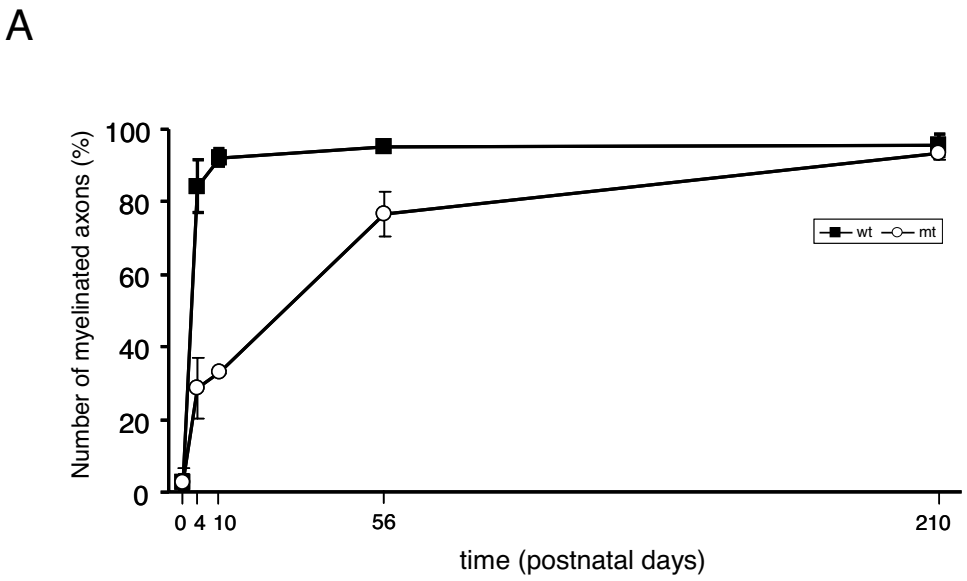

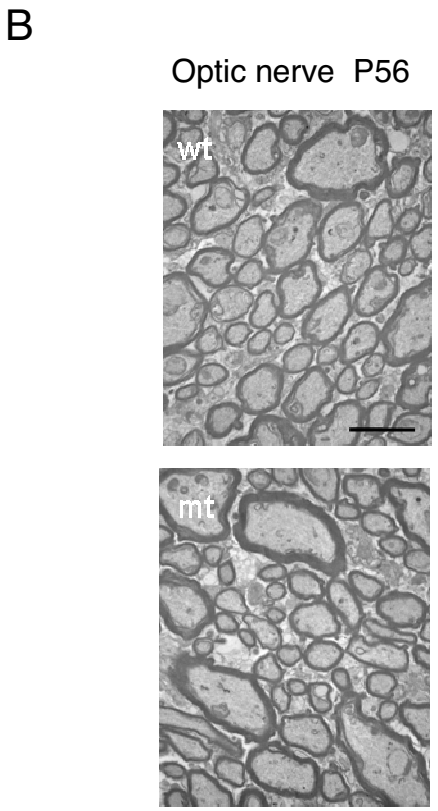

Fig. S3. (*A*) Quantification of reduced number of myelinated axons in SCAP mutant nerves. Shown is the percentage of myelinated axons of the total number of single axons at depicted time points (*B*) Electron microscopic analysis of optic nerve myelination in wild-type (wt) and mutant (mt) mice at P56. No differences were observed between wild-type and SCAP mutant CNS myelin. (Scale bar, 2.5 μm.)

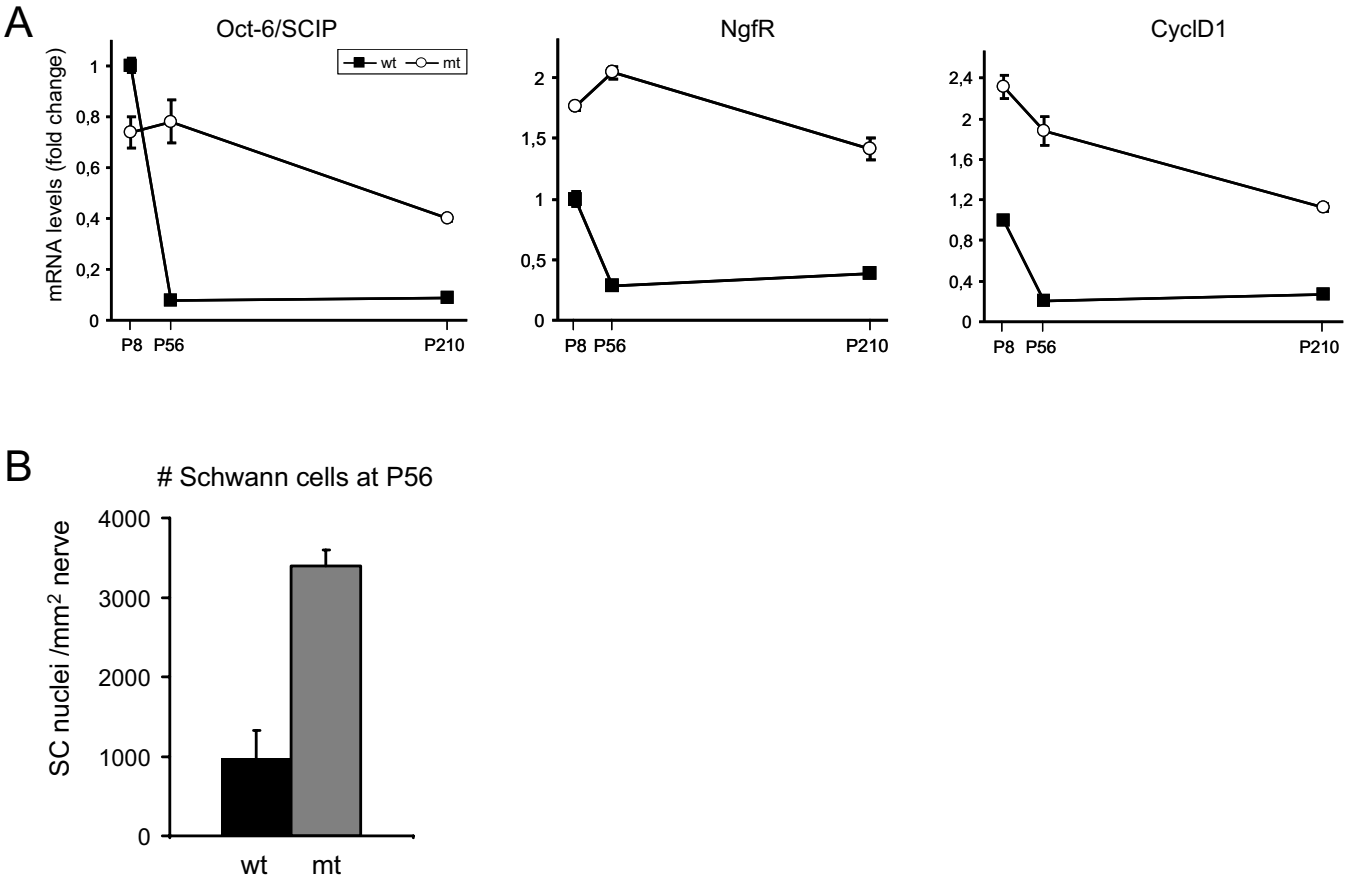

Fig. S4. Prolonged presence of immature Schwann cell phenotype in SCAP mutant nerves. (*A*) Quantitative PCR analysis of immature Schwann cell markers Oct-6/SCIP, NgfR and CyclinD1 mRNA levels in sciatic nerve endoneurium of wild-type (wt) versus mutant (mt) adult mice at depicted time points. The data represent the mean ± standard deviation of triplicate measurements. Expression level at time point P8 in wild-type sample was arbitrarily set to 1, and level in mutant sample was accordingly normalized. For all other time points, the mRNA levels are represented as fold increase over the mRNA expression level at P8. (*B*) The number of Schwann cell nuclei per mm^2 of nerve in wild-type (wt) versus mutant (mt) adult (P56) mice. The data represent the mean ± standard deviation of triplicate measurements.

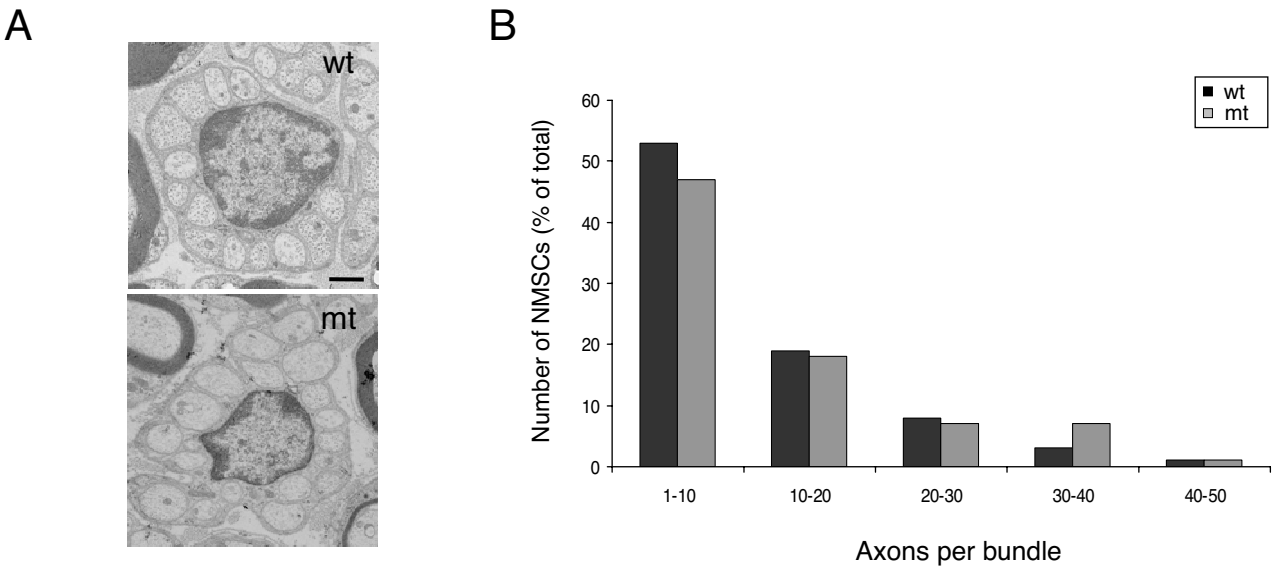

Fig. S5. Axon bundling by nonmyelinating Schwann cells is not affected in SCAP mutant nerves. (*A*) Electron micrograph of nonmyelinating Schwann cell bundles in wild-type (wt) and SCAP mutant (mt) sciatic nerves. [Scale bar, (mt) 1 μm; (wt) 0.78 μm.] (*B*) Morphometric analysis shows the number of axons per bundle of nonmyelinating Schwann cell for wild-type and SCAP mutant sciatic nerve at P56. The data represent the mean $\pm$ standard deviation of triplicate measurements.

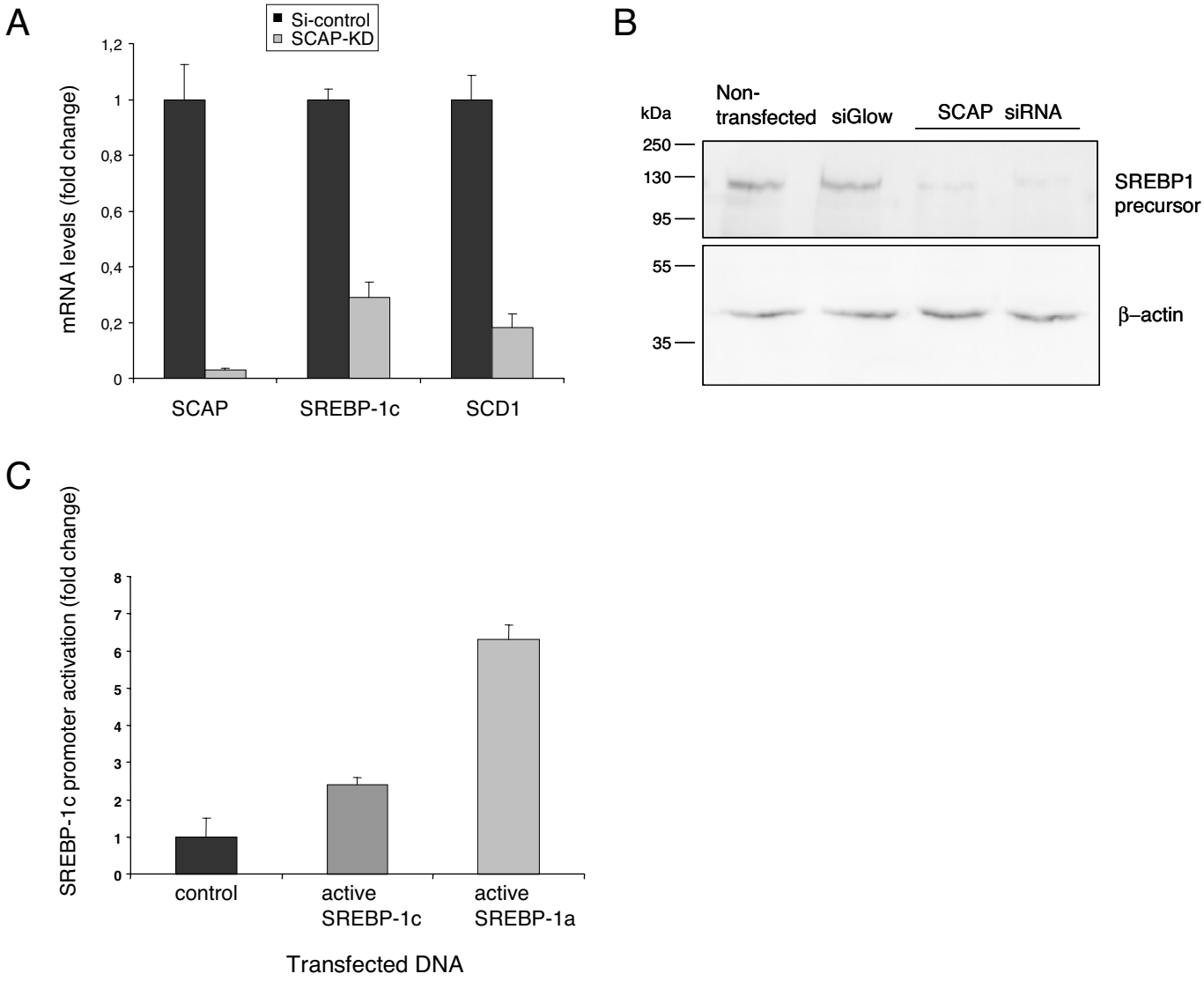

Fig. S6. SCAP deletion interferes with SREBP autoregulatory transcription in primary cultured Schwann cells. (*A*) Primary cultured Schwann cells were transfected with either siRNA directed against SCAP (SCAP-KD), or nontargeting siRNA (Si-control), and the effect on mRNA levels for SCAP, SREBP1c and SCD1 was measured by qPCR. Expression level in Si-control sample was arbitrarily set to 1 and level in SCAP-KD sample was normalized accordingly. (*B*) SREBP-1c precursor protein and β-actin were detected by immunoblot analysis in extracts of primary cultured Schwann cells that were nontransfected or transfected with either siRNA directed against SCAP, or nontargeting siRNA (siGLOW). (*C*) Primary cultured Schwann cells were transfected with a SREBP-1c promoter luciferase reporter construct and with or without a CMV-driven expression construct for an active form of SREBP-1c or SREBP-1a. (*A* and *C*) The data represent the mean $\pm$ standard deviation of three measurements.

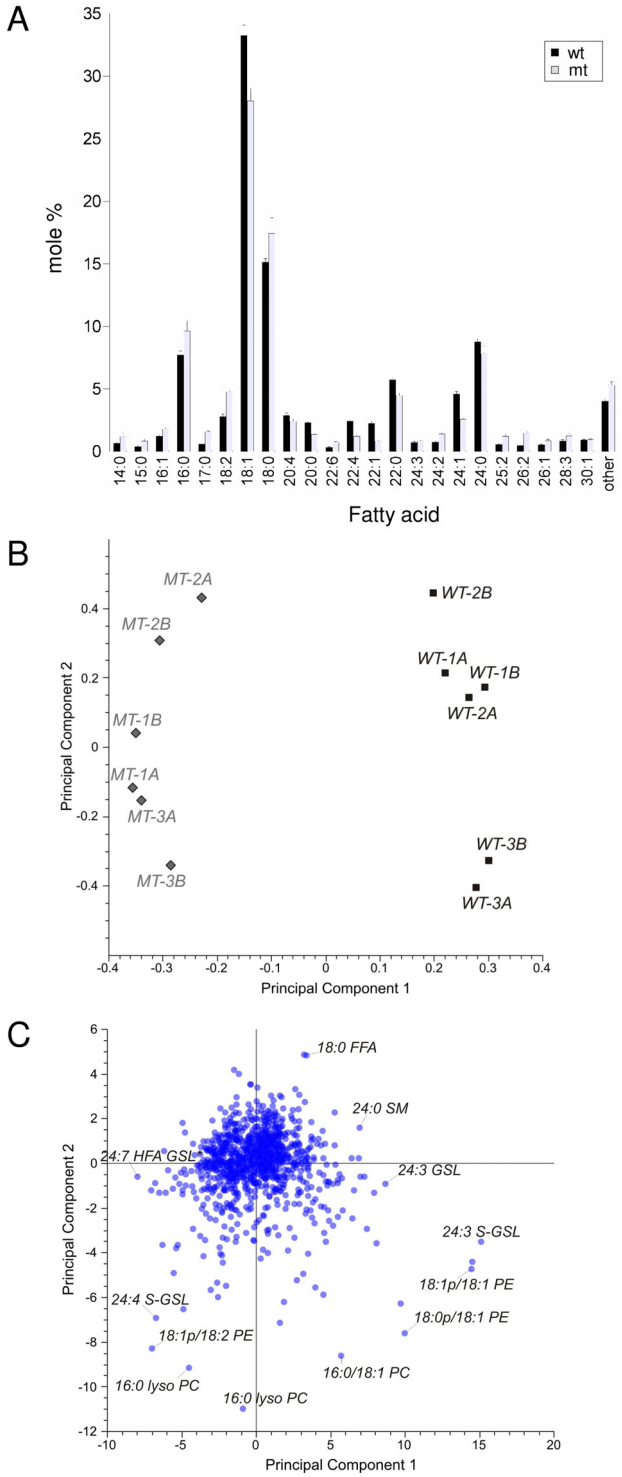

Fig. S7. SCAP deletion induces changes in fatty acid saturation and lipid species in myelin. (*A*) Depicted are the amounts of different fatty acid species as percentage of the total amount. The data represent the mean ± standard deviation of measurements on three animals per genotype. (*B*) Phospholipid species in lipid extracts of myelin of P210 wild-type (wt) or SCAP mutant (mt) mice were analyzed by using mass spectrometry. Analysis was done on three animals per genotype, and on two separate nerve samples per animal (nerve a and nerve b). The lipid composition of these 12 samples was analyzed by PCA, the first two coordinates (Principal Component 1 and Principal Component 2) together represent >77% of the variance of these 12 samples. Principal Component 1 represents 64% of this variance and clearly discriminates between mutant and wild-type myelin. (*C*) Lipid species that contribute the most to Principal Component 1 may be considered to be markers for either wild-type myelin (positive contribution to Principal Component 1) or mutant myelin (negative contribution to Principal Component 1). PE, phosphatidyl ethanolamine; SM, sphingomyelin; GSL, glycosphingolipid; S-GSL, Sulfatide GSL; and HFA GSL, alpha-hydroxy-fatty acid GSL.

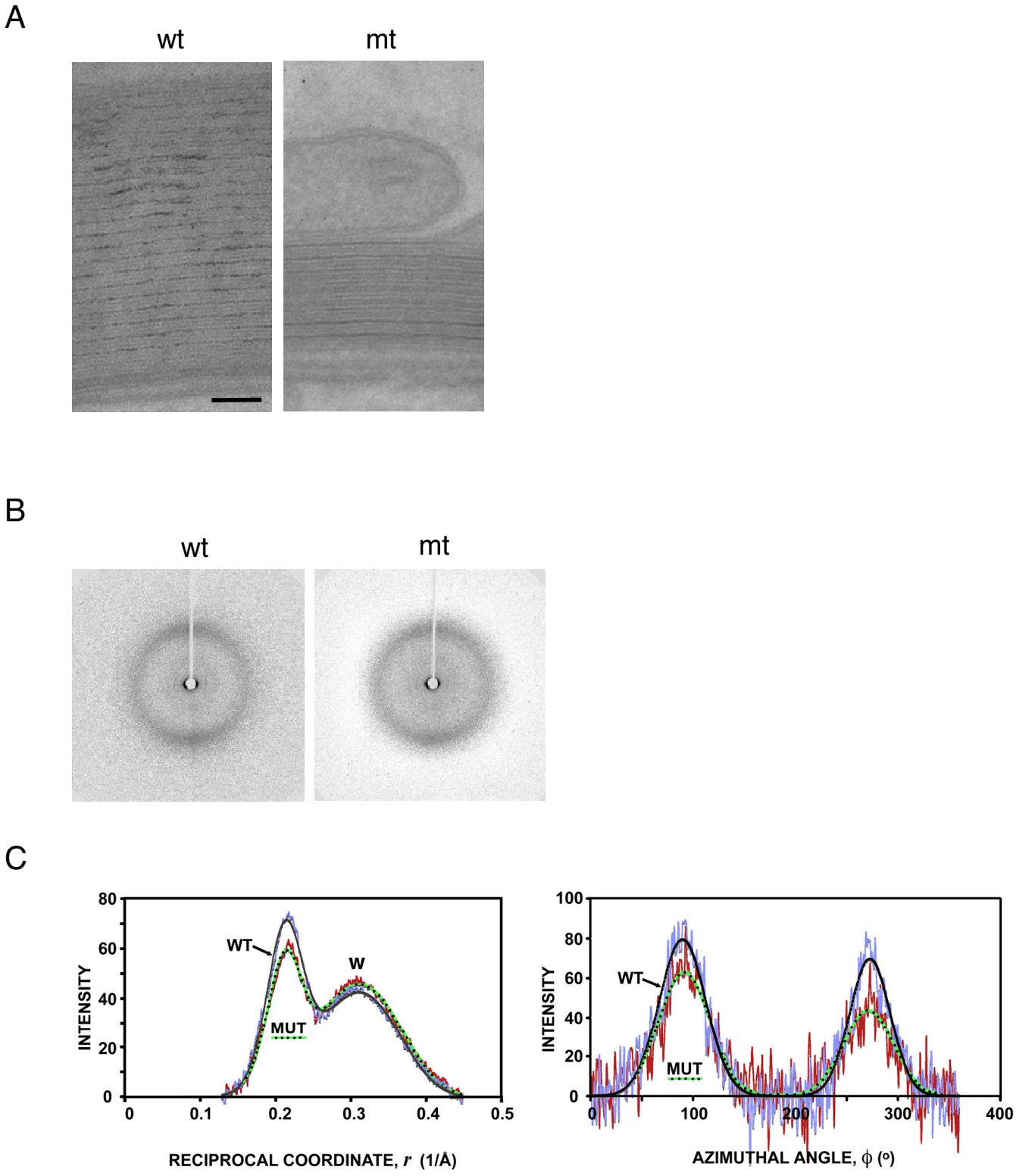

Fig. S8. SCAP deletion induces fine structural changes in peripheral nerve myelin. (*A*) Electron micrographs of wild-type (wt) and SCAP mutant (mt) myelin membranes of sciatic nerve at P4. Periodicity of myelin is not detectably affected in mutant mice. (Scale bar, 50 nm.) (*B*) Point-focus XRD analysis of myelin of wild-type and SCAP mutant optic nerves at P210 shows no significant changes. Quantifications are summarized in Fig. 5*F*. (*C*) Graphs show the quantified intensity of wide-angle scatter from the fatty acyl chains in the internodal PNS myelin, as depicted in Fig. 5*E*, measured on the reciprocal coordinate (*Left*) or in relation to the Azimuthal angle (*Right*).

Movie S1. Walking behavior of young adult (P56) wild-type mice.

Movie S1 (WMV)

Movie S2. Walking behavior of young adult (P56) SCAP mutant mice.

Movie S2 (WMV)

Movie S3. Walking behavior of old adult (P210) wild-type mice.

Movie S3 (WMV)

Movie S4. Walking behavior of old adult (P210) SCAP mutant mice.

Movie S4 (WMV)

Table S1. PCR primers

SCAP mutant mice genotyping	F1:	CCTCAGGGCAAGAGTGTCTC
	F2:	GGGTACGTCTTGCTTTGGAA
	R:	CAGCCGGCAAGTAACAAGGGATCCG
HMGCoARed	F:	TGA AGA GGA CGT GCT GAG CA
	R:	CAC CGC GTT ATC GTC AGG AT
FASN	F:	GGG TGC TGA CTA CAA CCT CTC C
	R:	TGC ACA GAC ACC TTC CCG TC
PMP22	F:	TTG CTC TTC GTC TCC ACC ATC
	R:	TCG TGT GTC CAT TGC CCA C
MAG	F:	TAG CGT TCC TCA GCT CCT CAT T
	R:	CTT TCA ACC AAG TCT CTT CAG GG
SREBP2	F:	CCC ACT CAG AAC ACC AAG CA
	R:	AGT AGC TCG CTC TCG TTG GC
SREBP1c	F:	GCCATGGATTGCACATTTGA
	R:	TGGTTGTTGATGAGCTGGAGC
SREBP1a	F:	GAA CAG ACA CTG GCC GAG ATG T
	R:	GGT TGT TGA TGA GCT GGA GCA T
SCAP	F:	CTG CTA CCC GCT GCT GAA
	R:	AGA ATT CCA CAG GTC CCG TTC
UBIQUITIN	F:	CAG CCA CCA AGA CTG ACC AA
	R:	CAT TCA CCA GTG CTA TGA GGG A
CYCLOPHILIN	F:	CCA TCG TGT CAT CAA GGA CTT C
	R:	CCC GTA GTG CTT CAG CTT GAA
UGT8a	F:	CAGAGGCGCTCTCCAACTC
	R:	GCACTCCACAGGAGCATGAA
NGFR	F:	GCTGCAAAGCCTGCAACCT
	R:	CGCTCACCACGTCAGAGAAC
Cyclin D1	F:	GCAGCCTGCCCACATCAG
	R:	CAGCAACACTGCCTCCAGCTA